

HER MAJESTY
ROYAL AIRCRAFT ESTABLISHMENT
REPORT



MINISTRY OF AVIATION

AERONAUTICAL RESEARCH COUNCIL

CURRENT PAPERS

The Calculation of Pressure Distribution
in Steady Supersonic Flow with
Arbitrary Downwash Distribution

By

Laura Klanfer, B.Sc.

LONDON: HER MAJESTY'S STATIONERY OFFICE

1965

PRICE 6s. 6d. NET

U.D.C. No. 533.693.3 : 533.6.048.2/.3 : 533.6.011.5

C.P. No. 703

April, 1963

THE CALCULATION OF PRESSURE DISTRIBUTION IN
STEADY SUPERSONIC FLOW, WITH ARBITRARY DOWNWASH DISTRIBUTION

by

Laura Klanfer, B.Sc.

SUMMARY

A method is established on the basis of linearized thin-wing theory for the calculation of pressure distribution, in steady supersonic flow, on wings of arbitrary planform with subsonic leading edges. An algebraic expression is derived by exact integration for the incidence contribution and a computational formula, based on Gaussian integration, is given for the general case including any prescribed camber and twist.

For a uniformly cambered delta wing the results computed by this method check very closely against those obtained by Watkins' method, which is applicable in this special case. As illustrated by results computed for an uncambered ogee wing the method appears to give results of more general application than slender body or first-order piston theory.

LIST OF CONTENTS

	<u>Page</u>
1 INTRODUCTION	4
2 BASIC EQUATIONS	5
3 INTEGRAL EXPRESSION FOR ΔC_p	9
4 PRESSURE DISTRIBUTION DUE TO INCIDENCE	13
5 NUMERICAL EVALUATION OF INTEGRALS	14
5.1 Integrals for 1st integration area	14
5.2 Integrals for 2nd integration area	15
5.3 Numerical expression for ΔC_p	16
6 APPLICATION	19
6.1 The cambered delta wing	19
6.2 The uncambered ogee wing	19
ACKNOWLEDGEMENT	20
LIST OF SYMBOLS	20
LIST OF REFERENCES	21
APPENDICES 1 AND 2	23-25
TABLE 1 - Integration points and interpolation coefficients for Gaussian integration	26
ILLUSTRATIONS - Figs.1-6	-
DETACHABLE ABSTRACT CARDS	-

LIST OF APPENDICES

Appendix

1 - Removal of singularity from double integral	23
2 - Calculation of tangents at points of intersection	24

LIST OF ILLUSTRATIONS

	<u>Fig.</u>
Integration areas for typical ogee wing	1
(a) $M = 1.2$	
(b) $M = 2.8$	
Notation for computation	2
Spanwise pressure distribution, delta wing	3
Chordwise pressure distribution, delta wing	4
Spanwise pressure distribution, ogee wing	5
Chordwise pressure distribution, ogee wing	6

1 INTRODUCTION

The application of linearized theory to supersonic flow over wings has been widely developed and has led to satisfactory solutions of many features of aircraft design. However, for those aerodynamic and aeroelastic aspects of design which demand reliable estimates of lift distribution, existing methods are all subject to limitations and may give rise to difficulties or uncertainties in the general case.

Within the limit of its range of application $[A^2]1 - M^2 \ll 1$ slender body theory¹ can be applied to indicate the main trends of the aerodynamic properties of wings in supersonic flow. For speeds in excess of, say, $M = 2.0$, piston theory² can provide useful and very simply derived results, especially in the approximate evaluation of aeroelastic properties.

A formal representation of the problem of a wing in supersonic flow can be made in terms of a distribution of sources with strength proportional to local downwash, the effects being bounded by Mach lines. For a surface with supersonic edges the system can be formulated fairly simply, but complications arise in the case of subsonic edges, because the effective areas include parts not on the wing, where the downwash is generally unknown. Tractable expressions have been derived for the computation of velocity potential and lift force at points on rigid and deforming wings of basically triangular planform in both steady and oscillatory states^{3,4,5}.

A general approach to the problem of subsonic edges was propounded by Evvard⁶. Velocity potential at any point requires integration of the downwash velocity effect over the area enclosed by the Mach lines from the apex of the wing and the reversed Mach lines through the point under consideration. Evvard prescribes a portion of the wing area to cancel the effect of that part of the original integration area which lies outside the wing itself.

In a development of this method Etkin⁷ showed that this area cancellation could be improved by using a series of integration areas, of appropriate sign, defined by reversed Mach lines through the point and through successive intersections of these Mach lines with the wing edges. In the limiting case of sonic leading edges a single integration area gives the exact solution; for subsonic edges one, two or more areas of diminishing influence may be used to achieve successive degrees of approximation. Evvard and Etkin calculate the velocity potential by numerical integration, and use numerical differentiation for pressure.

Lees⁸ describes a routine numerical procedure based on a matrix application of influence coefficients calculated for elements of an equispaced Mach line grid. He avoids numerical differentiation by line integration round each elementary panel. Downwash and pressure are assumed to have uniform mean values over each panel.

In the present paper a convenient method is evolved for the application of a general solution of aerodynamic loadings on wings with subsonic leading edges, having arbitrary, specified planform and downwash distribution. Using Etkin's integration areas, it can be shown that a useful range of shapes and Mach numbers

can be approximated quite closely by taking only two such areas. Under these conditions it is shown that an analytical formulation can be derived by differentiation in the chordwise direction of the integral expression for the velocity potential. The resulting expressions for pressure distribution at any point is the sum of integrals of known functions over the appropriate areas. These integrals can be evaluated exactly for the contribution of incidence to pressure and by Gaussian integration methods for the general case.

The integrations have been programmed for the Mercury computer for the evaluation of pressure at points along chord lines on wings for which the leading edges may be specified as polynomial functions. For the same basic wing shape, different distributions of downwash are readily introduced.

Confirmation of the accuracy of the method is accorded by very close agreement with Watkins' method³, as given by Davies⁵, which is applicable to the particular case chosen for the comparison. This was a uniformly cambered delta wing of aspect ratio 1.0 at a Mach number of 2.0, for which the results may be interpreted in terms of an uncambered wing in steady pitch.

An uncambered ogee wing of aspect ratio 1.0, used by Courtney and Ormerod⁹, for the experimental determination of pressure distribution was also examined. Over the speed range considered - Mach numbers from 1.4 to 2.8 - the present method appears to be more generally applicable than either slender-body theory or first-order piston theory.

The experimental evidence is that leading-edge separation and vortex formation is a feature of each of the cases considered. Thus the degree of correlation between measured and theoretically derived pressures cannot be applied to the assessment of theories which themselves assume, and are strictly applicable only in cases of completely attached flow. It is noted, however, that in those cases where separation effects are least (high speed, low incidence, inboard) the present method of computation gives results which agree quite well with observed pressures. While it is unsafe to generalise from one example this is at least an indication that, for practical purposes, the present method might be admissible and useful for cases which involve only small departures from conditions of attached flow.

Summarising, the analytical and computational techniques described here should prove useful in the study of aerodynamic and steady-state aeroelastic properties of wings in supersonic flow, over the region where linearized thin-wing theory is applicable. For stability and dynamics studies the computed pressure due to incidence may be used directly to determine supersonic wing derivatives z_w and m_w ; downwash distributions proportional to longitudinal and lateral coordinates may be applied to give 'q' and 'p' derivatives respectively.

2 BASIC EQUATIONS

We assume a wing placed in supersonic steady flow of free-stream velocity V , and choose a Cartesian coordinate system with origin at the apex of the wing, x-axis along the centre line of the wing in the direction of the main stream flow, y-axis in the starboard direction and z-axis positive downwards.

The perturbation velocity potential at a point $P(x_0, y_0)$ on the wing is then given by Evvard⁶ as

$$\phi(x_0, y_0) = -\frac{1}{\pi} \iint \frac{w(x, y) \, dx \, dy}{\sqrt{(x_0 - x)^2 - \beta^2(y_0 - y)^2}} \quad (1)$$

where $\beta = \sqrt{M^2 - 1}$ and downwash velocity $w(x, y)$ is $V \frac{\partial z}{\partial x}$ for points on the wing surface.

The area of integration is enclosed by the reversed Mach lines through P and Mach lines through the apex of the wing. In the case of subsonic leading edges the downwash velocity is not known for that part of the area which is not on the wing, but Evvard⁶ and Etkin⁷ have shown that the integration area can be replaced by a system of areas on the wing surface. Areas A_1, A_2, A_3, \dots which are bounded by reversed Mach lines through P and through successive intersections of such Mach lines with the wing edges, as shown in Fig. 1, may be used for approximate calculations.

Etkin estimated that, for delta wings, good accuracy is obtained if the integration is taken over the first area only, provided that $\beta \cot \Lambda \geq 0.4$, Λ being the angle of sweep-back; and also that the inclusion of the second area is sufficient in most cases.

For a near delta wing of aspect ratio 1.0 at Mach numbers close to unity it is clear (Fig. 1a, $M = 1.2$) that even areas A_3 and A_4 are not negligible. At such Mach numbers, however, the flow would be transonic in character and the theory unlikely to be reliable. As Mach number is increased the secondary areas become smaller, and at $M = 2.8$ (Fig. 1b) it can be seen that A_2 is quite small for a typical slender wing. At a Mach number of about 4.1 the leading edge of this wing becomes supersonic and A_2 vanishes; here, however, we are approaching the hypersonic regime.

It will be seen from this that for slender wings in supersonic flow it will be necessary only to deal with the case of subsonic leading edges and that two integration areas will give a good approximation for $M > 1.4$, say. Under these conditions the equation for velocity potential becomes:-

$$\phi(x_0, y_0) = -\frac{1}{\pi} \iint_{A_1} \frac{w(x, y) \, dx \, dy}{\sqrt{(x_0 - x)^2 - \beta^2(y_0 - y)^2}} + \frac{1}{\pi} \iint_{A_2} \frac{w(x, y) \, dx \, dy}{\sqrt{(x_0 - x)^2 - \beta^2(y_0 - y)^2}} \dots \quad (2)$$

The linearized form of Bernoulli's equation is

$$\frac{p - p_o}{\rho} + V \frac{\partial \phi}{\partial x} = 0 . \quad (3)$$

For a thin wing, the pressure difference between upper and lower surfaces may be written

$$p_\ell - p_u = 2\rho V \left(\frac{\partial \phi}{\partial x} \right)_u$$

or

$$\Delta C_p = \frac{p_\ell - p_u}{\frac{1}{2}\rho V^2} = \frac{4}{V} \left(\frac{\partial \phi}{\partial x} \right)_u . \quad (4)$$

Introducing characteristic coordinates (r, s) based on the Mach lines through the apex of the wing, we have

$$\left. \begin{aligned} r &= \frac{M}{2\beta} (x - \beta y) \\ s &= \frac{M}{2\beta} (x + \beta y) . \end{aligned} \right\} \quad (5)$$

Transforming equation (2) into this system, we obtain

$$\begin{aligned} \phi(x_o, y_o) &= \bar{\phi}(r_o, s_o) \\ &= -\frac{1}{\pi M} \iint_{A_1} \frac{W(r, s) dr ds}{\sqrt{(r_o - r)(s_o - s)}} + \frac{1}{\pi M} \iint_{A_2} \frac{W(r, s) dr ds}{\sqrt{(r_o - r)(s_o - s)}} \end{aligned} \quad (6)$$

$$= -\frac{1}{\pi M} [I_1 - I_2] \quad (6a)$$

where I_1 and I_2 represent the integrals over areas A_1 and A_2 .

Now

$$\begin{aligned}
 \frac{\partial \varphi(x, y)}{\partial x} &= \frac{\partial \Phi(r, s)}{\partial x} \\
 &= \frac{\partial \Phi}{\partial r} \frac{\partial r}{\partial x} + \frac{\partial \Phi}{\partial s} \frac{\partial s}{\partial x} \\
 &= \frac{M}{2\beta} \left[\frac{\partial \Phi}{\partial r} + \frac{\partial \Phi}{\partial s} \right]. \tag{7}
 \end{aligned}$$

Thus, we may write, using (4), (7) and (6a),

$$\begin{aligned}
 \Delta C_p(x_0, y_0) &= \frac{4}{V} \frac{\partial \varphi(x_0, y_0)}{\partial x_0} \\
 &= \frac{2M}{\beta V} \left[\frac{\partial \Phi(r_0, s_0)}{\partial r_0} + \frac{\partial \Phi(r_0, s_0)}{\partial s_0} \right] \\
 &= -\frac{2}{\pi\beta V} \left[\frac{\partial}{\partial r_0} (I_1 - I_2) + \frac{\partial}{\partial s_0} (I_1 - I_2) \right] \tag{8}
 \end{aligned}$$

or, on rearranging:-

$$\left. \begin{aligned}
 \left(\frac{\partial I_1}{\partial r_0} - \frac{\partial I_2}{\partial r_0} \right) + \left(\frac{\partial I_1}{\partial s_0} - \frac{\partial I_2}{\partial s_0} \right) &= -\pi M \left[\frac{\partial \Phi}{\partial r_0} + \frac{\partial \Phi}{\partial s_0} \right] \\
 &= -2\pi\beta \frac{\partial \varphi(x_0, y_0)}{\partial x_0} \\
 &= -\frac{\pi\beta V}{2} \Delta C_p(x_0, y_0).
 \end{aligned} \right\} \tag{8a}$$

Thus, to evaluate ΔC_p we must determine partial derivatives, with respect to r_0 and s_0 , of the integral expressions for Φ .

3 INTEGRAL EXPRESSION FOR Δ_C _P

Following the notation of Fig.2, and using the definitions in equation (6a), we may write

$$\left. \begin{aligned} I_1 &= \int_{r=r_0}^{r_1} \int_{s=s_0}^{s_1} \frac{W(r,s)}{\sqrt{(r_0-r)(s_0-s)}} dr ds \\ I_2 &= \int_{r=r_1}^{r_2} \int_{s=s_1}^{s_2} \frac{W(r,s)}{\sqrt{(r_0-r)(s_0-s)}} dr ds . \end{aligned} \right\} \quad (9)$$

It will be seen from Fig.2 that r_2 and s_1 are functions of r_0 , but that s_0 , r_1 and s_2 are not. In differentiating with respect to r_0 , consider a point $P_1(t, s_0)$ passing to the limit at $P(r_0, s_0)$, so that t is also a function of r_0 . We now differentiate the integral J_1 , defined by

$$J_1 = \int_t^{r_1} \int_{s_0}^{s_1} \frac{W(r,s) dr ds}{\sqrt{(r_0-r)(s_0-s)}} = \int_t^{r_1} \int_{s_0}^{s_1} f_1(r,s) dr ds .$$

This becomes¹⁰

$$\begin{aligned} \frac{\partial J_1}{\partial r_0} &= \int_{s_0}^{s_1} ds \int_t^{r_1} \frac{\partial f_1}{\partial r_0} dr + \frac{ds_1}{dr_0} \int_t^{r_1} f_1(r, s_1) dr - \frac{dt}{dr_0} \int_{s_0}^{s_1} f_1(t, s) ds \\ &= -\frac{1}{2} \int_{s_0}^{s_1} \frac{ds}{\sqrt{s_0-s}} \int_t^{r_1} \frac{W(r,s) dr}{(r_0-r)^{3/2}} + \frac{\frac{ds_1}{dr_0}}{\sqrt{s_0-s_1}} \int_t^{r_1} \frac{W(r, s_1) dr}{\sqrt{r_0-r}} - \frac{\frac{dt}{dr_0}}{\sqrt{r_0-t}} \int_{s_0}^{s_1} \frac{W(t, s) ds}{\sqrt{s_0-s}} . \end{aligned}$$

... (10)

In order to remove the singularity, this expression may be rearranged (Appendix 1) as:-

$$\begin{aligned}
\frac{\partial J_1}{\partial r_0} = & -\frac{1}{2} \int_{s_0}^{s_1} \frac{ds}{\sqrt{s_0 - s}} \int_t^{r_1} \frac{\left[W(r,s) - \frac{dt}{dr_0} W(t,s) \right] dr}{(r_0 - r)^{3/2}} + \\
& + \frac{\frac{ds_1}{dr_0}}{\sqrt{s_0 - s_1}} \int_t^{r_1} \frac{W(r,s_1) dr}{\sqrt{r_0 - r}} - \frac{\frac{dt}{dr_0}}{\sqrt{r_0 - r_1}} \int_{s_0}^{s_1} \frac{W(t,s) ds}{\sqrt{s_0 - s}} .
\end{aligned}
\tag{11}$$

The equation of the port leading edge may be written in characteristic coordinates as

$$s = g(r).$$

The slope at point R (Fig.2) is

$$\frac{ds_1}{dr_0} = g'(r_0).$$

Proceeding now to the limit where $t = r_0$ so that $dt/dr_0 \rightarrow 1$, we have

$$\begin{aligned}
\frac{\partial I_1}{\partial r_0} = & \lim_{t \rightarrow r_0} \frac{\partial J_1}{\partial r_0} \\
= & -\frac{1}{2} \int_{s_0}^{s_1} \frac{ds}{\sqrt{s_0 - s}} \int_{r_0}^{r_1} \frac{[W(r,s) - W(r_0,s)] dr}{(r_0 - r)^{3/2}} + \frac{g'(r_0)}{\sqrt{s_0 - s_1}} \int_{r_0}^{r_1} \frac{W(r,s_1) dr}{\sqrt{r_0 - r}} \\
& - \frac{1}{\sqrt{r_0 - r_1}} \int_{s_0}^{s_1} \frac{W(r_0,s) ds}{\sqrt{s_0 - s}} .
\end{aligned}
\tag{12}$$

Differentiation of the corresponding expression for I_2 can be carried out directly as there is no singularity. Noting that the starboard leading edge is given by

$$r = g(s)$$

and that

$$\frac{dr_2}{ds_1} = g'(s_1)$$

we have

$$\begin{aligned} \frac{dr_2}{dr_0} &= \frac{dr_2}{ds_1} \frac{ds_1}{dr_0} \\ &= g'(s_1)g'(r_0) \end{aligned}$$

and we find

$$\begin{aligned} \frac{\partial I_2}{\partial r_0} &= -\frac{1}{2} \int_{s_1}^{s_2} \frac{ds}{\sqrt{s_0-s}} \int_{r_1}^{r_2} \frac{W(r,s)dr}{(r_0-r)^{3/2}} - \frac{g'(r_0)}{\sqrt{s_0-s_1}} \int_{r_1}^{r_2} \frac{W(r,s_1)dr}{\sqrt{r_0-r}} \\ &\quad + \frac{g'(s_1)g'(r_0)}{\sqrt{r_0-r_2}} \int_{s_1}^{s_2} \frac{W(r_2,s)ds}{\sqrt{s_0-s}}. \end{aligned} \quad (13)$$

Thus,

$$\begin{aligned} -\pi M \frac{\partial \Phi}{\partial r_0} &= \frac{\partial I_1}{\partial r_0} - \frac{\partial I_2}{\partial r_0} \\ &= -\frac{1}{2} \int_{s_0}^{s_1} \frac{ds}{\sqrt{s_0-s}} \int_{r_0}^{r_1} \frac{[W(r,s) - W(r_0,s)]dr}{(r_0-r)^{3/2}} + \frac{g'(r_0)}{\sqrt{s_0-s_1}} \int_{r_0}^{r_1} \frac{W(r,s_1)dr}{\sqrt{r_0-r}} \\ &\quad - \frac{1}{\sqrt{r_0-r_1}} \int_{s_0}^{s_1} \frac{W(r_0,s)ds}{\sqrt{s_0-s}} + \frac{1}{2} \int_{s_1}^{s_2} \frac{ds}{\sqrt{s_0-s}} \int_{r_1}^{r_2} \frac{W(r,s)dr}{(r_0-r)^{3/2}} \\ &\quad + \frac{g'(r_0)}{\sqrt{s_0-s_1}} \int_{r_1}^{r_2} \frac{W(r,s_1)dr}{\sqrt{r_0-r}} - \frac{g'(s_1)g'(r_0)}{\sqrt{r_0-r_2}} \int_{s_1}^{s_2} \frac{W(r_2,s)ds}{\sqrt{s_0-s}}. \end{aligned} \quad (14)$$

In the same way, taking the limit in the s-direction, we obtain:-

$$\begin{aligned}
 -\pi M \frac{\partial \Phi}{\partial s_0} &= -\frac{1}{2} \int_{r_0}^{r_1} \frac{dr}{\sqrt{r_0-r}} \int_{s_0}^{s_1} \frac{[W(r,s) - W(r,s_0)] ds}{(s_0-s)^{3/2}} + \frac{g'(s_0)}{\sqrt{r_0-r_1}} \int_{s_0}^{s_1} \frac{W(r_1,s) ds}{\sqrt{s_0-s}} \\
 &\quad - \frac{1}{\sqrt{s_0-s_1}} \int_{r_0}^{r_1} \frac{W(r,s_0) dr}{\sqrt{r_0-r}} + \frac{1}{2} \int_{r_1}^{r_2} \frac{dr}{\sqrt{r_0-r}} \int_{s_1}^{s_2} \frac{W(r,s) ds}{(s_0-s)^{3/2}} \\
 &\quad + \frac{g'(s_0)}{\sqrt{r_0-r_1}} \int_{s_1}^{s_2} \frac{W(r_1,s) ds}{\sqrt{s_0-s}} - \frac{g'(r_1)g'(s_0)}{\sqrt{s_0-s_2}} \int_{r_1}^{r_2} \frac{W(r,s_2) dr}{\sqrt{r_0-r}} . \quad (15)
 \end{aligned}$$

Combining equations (14) and (15) we obtain as the final equation for the calculation of pressure difference:-

$$\begin{aligned}
 -\frac{\pi \beta V}{2} \Delta C_p &= -2\pi \beta \frac{\partial \Phi}{\partial x} \\
 &= -\pi M \left(\frac{\partial \Phi}{\partial r_0} + \frac{\partial \Phi}{\partial s_0} \right) \\
 &= -\frac{1}{2} \int_{s_0}^{s_1} \frac{ds}{\sqrt{s_0-s}} \int_{r_0}^{r_1} \frac{[W(r,s) - W(r_0,s)] dr}{(r_0-r)^{3/2}} + \frac{g'(r_0)}{\sqrt{s_0-s_1}} \int_{r_0}^{r_1} \frac{W(r,s_1) dr}{\sqrt{r_0-r}} \\
 &\quad - \frac{1}{\sqrt{r_0-r_1}} \int_{s_0}^{s_1} \frac{W(r_0,s) ds}{\sqrt{s_0-s}} + \frac{1}{2} \int_{s_1}^{s_2} \int_{r_1}^{r_2} \frac{W(r,s) dr ds}{(r_0-r)^{3/2} (s_0-s)^{1/2}} \\
 &\quad + \frac{g'(r_0)}{\sqrt{s_0-s_1}} \int_{r_1}^{r_2} \frac{W(r,s_1) dr}{\sqrt{r_0-r}} - \frac{g'(s_1)g'(r_0)}{\sqrt{r_0-r_2}} \int_{s_1}^{s_2} \frac{W(r_2,s) ds}{\sqrt{s_0-s}} \\
 &\quad - \frac{1}{2} \int_{r_0}^{r_1} \frac{dr}{\sqrt{r_0-r}} \int_{s_0}^{s_1} \frac{[W(r,s) - W(r,s_0)] ds}{(s_0-s)^{3/2}} + \frac{g'(s_0)}{\sqrt{r_0-r_1}} \int_{s_0}^{s_1} \frac{W(r_1,s) ds}{\sqrt{s_0-s}}
 \end{aligned}$$

$$\begin{aligned}
& - \frac{1}{\sqrt{s_0 - s_1}} \int_{r_0}^{r_1} \frac{W(r, s_0) dr}{\sqrt{r_0 - r}} + \frac{1}{2} \int_{s_1}^{s_2} \int_{r_1}^{r_2} \frac{W(r, s) dr ds}{(r_0 - r)^{1/2} (s_0 - s)^{3/2}} \\
& + \frac{g'(s_0)}{\sqrt{r_0 - r_1}} \int_{s_1}^{s_2} \frac{W(r_1, s) ds}{\sqrt{s_0 - s}} - \frac{g'(r_1)g'(s_0)}{\sqrt{s_0 - s_2}} \int_{r_1}^{r_2} \frac{W(r, s_2) dr}{\sqrt{r_0 - r}} . \quad (16)
\end{aligned}$$

4. PRESSURE DISTRIBUTION DUE TO INCIDENCE

When calculating the pressure distribution over a cambered and twisted wing at incidence according to linearized theory, the contributions of camber, twist and incidence may be calculated separately and the results superimposed. The pressure distribution due to incidence is calculated per radian with $\frac{W}{V} = 1$. This leads to a considerable simplification of equation (16), since in that case $W(r, s) - W(r_0, s) = 0$ and $W(r, s) - W(r, s_0) = 0$ so that the two double integrals over the area A_1 vanish. The other integrals can be evaluated exactly. We thus obtain for the pressure distribution due to incidence:-

$$\begin{aligned}
- \frac{\beta\pi}{4} \Delta C_p &= - \frac{\beta\pi}{V} \frac{\partial\phi}{\partial x} \\
&= \left\{ 1 - g'(r_0) \right\} \frac{\sqrt{r_0 - r_2}}{\sqrt{s_0 - s_1}} + \left\{ g'(s_1)g'(r_0) - 1 \right\} \frac{\sqrt{s_0 - s_2}}{\sqrt{r_0 - r_2}} \\
&\quad + \left\{ 1 - g'(s_1)g'(r_0) \right\} \frac{\sqrt{s_0 - s_1}}{\sqrt{r_0 - r_2}} + \left\{ 1 - g'(s_0) \right\} \frac{\sqrt{s_0 - s_2}}{\sqrt{r_0 - r_1}} \\
&\quad + \left\{ g'(r_1)g'(s_0) - 1 \right\} \frac{\sqrt{r_0 - r_2}}{\sqrt{s_0 - s_2}} + \left\{ 1 - g'(r_1)g'(s_0) \right\} \frac{\sqrt{r_0 - r_1}}{\sqrt{s_0 - s_2}} . \\
&\quad \dots (17)
\end{aligned}$$

This is all we have to calculate for a wing without camber or twist, or in determining the contribution of incidence in the general case.

5 NUMERICAL EVALUATION OF THE INTEGRALS

The integrals of equation (16) were evaluated by Gaussian integration which involves only the summation of terms containing $W(r,s)$ at selected integration points. The double integrals are calculated as repeated single integrals.

5.1 Integrals for the integration area A_1

To evaluate the first integral of equation (16) we make the transformation

$$u = \frac{r_0 - r}{r_0 - r_1}, \quad v = \frac{s_0 - s}{s_0 - s_1},$$

that is, we make the coordinates non-dimensional with the sides of the area A_1 . This gives

$$r = r_0 - (r_0 - r_1)u, \quad dr = -(r_0 - r_1)du$$

and we obtain

$$\begin{aligned} & -\frac{1}{2} \int_{s_0}^{s_1} \frac{ds}{\sqrt{s_0 - s}} \int_{r_0}^{r_1} \frac{[W(r,s) - W(r_0,s)] dr}{(r_0 - r)^{3/2}} \\ &= -\frac{\sqrt{s_0 - s_1}}{2} \int_0^1 \frac{dv}{\sqrt{v}} \frac{(r_0 - r_1)}{(r_0 - r_1)^{3/2}} \int_0^1 \frac{[W(r_0 - (r_0 - r_1)u, s_0 - (s_0 - s_1)v) - W(r_0, s_0 - (s_0 - s_1)v)] du}{u^{3/2}} \\ &= -\frac{1}{2} \frac{\sqrt{s_0 - s_1}}{\sqrt{r_0 - r_1}} \sum_{k=1}^n H_k \int_0^1 \frac{[W(r_0 - (r_0 - r_1)u, s_0 - (s_0 - s_1)x_k) - W(r_0, s_0 - (s_0 - s_1)x_k)] du}{u^{3/2}} \\ &= -\frac{1}{2} \sqrt{\frac{s_0 - s_1}{r_0 - r_1}} \sum_{k=1}^n \sum_{i=1}^n \frac{H_k H_i}{x_i} \left[W(r_0 - (r_0 - r_1)x_i, s_0 - (s_0 - s_1)x_k) - W(r_0, s_0 - (s_0 - s_1)x_k) \right]. \end{aligned}$$

The values for the integration point x_i and the coefficients H_i were taken from Mineur¹¹ based on a formula given on page 289

$$J = \int_a^b \frac{F(x)}{\sqrt{b-x}} dx$$

$$I = \sqrt{b-a} [H_0 F(X_0) + \dots + H_n F(X_n)]$$

$$X_k = a + (b-a)\xi_k, \text{ where } x_k = 1 - \xi_k.$$

5.2 Integrals for the integration area A_2

In this case we make the coordinates non-dimensional with the sides of the area A_2 and put

$$u = \frac{r_1 - r}{r_1 - r_2}, \quad v = \frac{s_1 - s}{s_1 - s_2}.$$

This gives
$$r = r_1 - (r_1 - r_2)u$$

$$dr = - (r_1 - r_2)du$$

and
$$r_0 - r = (r_0 - r_1) + (r_1 - r_2)u.$$

We apply this transformation to the evaluation of the double integral

$$\begin{aligned} & \frac{1}{2} \int_{s_1}^{s_2} \int_{r_1}^{r_2} \frac{W(r,s) dr ds}{(s_0 - s)^{1/2} (r_0 - r)^{3/2}} \\ &= \frac{1}{2} (r_1 - r_2)(s_1 - s_2) \int_0^1 \int_0^1 \frac{W(r_1 - (r_1 - r_2)u, s_1 - (s_1 - s_2)v) du dv}{\{(s_0 - s_1) + (s_1 - s_2)v\}^{1/2} \{(r_0 - r_1) + (r_1 - r_2)u\}^{3/2}} \\ &= \frac{1}{2} (r_1 - r_2)(s_1 - s_2) \sum_{i=1}^n \sum_{k=1}^n G_i G_k \frac{W(r_1 - (r_1 - r_2)z_i, s_1 - (s_1 - s_2)z_k)}{\{(s_1 - s_2)z_k + (s_0 - s_1)\}^{1/2} \{(r_1 - r_2)z_i + (r_0 - r_1)\}^{3/2}}. \end{aligned}$$

The values of G_i and z_i were also taken from Mineur¹¹, based in this case on a different formula given on page 263

$$J = \int_a^b F(X) dX$$

$$I = \frac{(b-a)}{2} [G_0 F(X_0) + \dots + G_n F(X_n)]$$

$$X_k = \frac{b+a}{2} + \frac{(b-a)\zeta_k}{2}$$

where $z_k = 1 - \zeta_k$.

The values for x_i , H_i , z_i and G_i as used are given in Table 1.

5.3 Numerical expression for ΔC_p

With Gaussian integration applied to all integrals of equation (16) the final formula for the calculation of pressure distribution including camber and twist becomes the expression given in equation (18) on pages 17 and 18.

This expression with $n = 6$ was programmed for the Mercury computer for wings of arbitrary planform, the leading edge being given by a polynomial equation. With the value $n = 6$, there are 36 integration points in each area for every point. It thus provides automatically for greater accuracy near the leading edge since the same number of integration points are used for smaller areas.

In the programme, the calculation is carried out for points along chord lines equi-distant in Cartesian coordinates and is so arranged that only the downwash distribution has to be added for each new case of camber or twist.

As the leading edges are usually specified in Cartesian coordinates, formulae are given in Appendix 2 for evaluation of the terms $g'(r_0)$ etc. without requiring to express the equations for the leading edges explicitly in characteristic coordinates.

$$-\frac{\pi\beta V}{2} \Delta C_p = -2\pi\beta \frac{\partial \phi}{\partial x}$$

$$\begin{aligned}
&= \sqrt{\frac{s_0 - s_1}{r_0 - r_1}} \left[\sum_{k=1}^n H_k W(r_0, s_0 - (s_0 - s_1)x_k) \right. \\
&\quad \left. - \frac{1}{2} \sum_{i=1}^n \sum_{k=1}^n \frac{H_i H_k}{x_i} \left\{ W(r_0 - (r_0 - r_1)x_i, s_0 - (s_0 - s_1)x_k) - W(r_0, s_0 - (s_0 - s_1)x_k) \right\} \right] \\
&+ \sqrt{\frac{r_0 - r_1}{s_0 - s_1}} \left[\sum_{k=1}^n H_k W(r_0 - (r_0 - r_1)x_k, s_0) \right. \\
&\quad \left. - \frac{1}{2} \sum_{k=1}^n \sum_{i=1}^n \frac{H_k H_i}{x_k} \left\{ W(r_0 - (r_0 - r_1)x_i, s_0 - (s_0 - s_1)x_k) - W(r_0 - (r_0 - r_1)x_i, s_0) \right\} \right] \\
&+ \frac{1}{2} (s_1 - s_2)(r_1 - r_2) \sum_{i=1}^n \sum_{k=1}^n G_{ik} \frac{W(r_1 - (r_1 - r_2)z_i, s_1 - (s_1 - s_2)z_k)}{\{(s_1 - s_2)z_k + (s_0 - s_1)\}^{3/2} \{(r_1 - r_2)z_i + (r_0 - r_1)\}^{1/2}}
\end{aligned}$$

$$\begin{aligned}
& + \frac{1}{2} (s_1 - s_2)(r_1 - r_2) \sum_{i=1}^n \sum_{k=1}^n G_i G_k \frac{W(r_1 - (r_1 - r_2)z_i, s_1 - (s_1 - s_2)z_k)}{\{(s_1 - s_2)z_k + (s_0 - s_1)\}^{1/2} \{(r_1 - r_2)z_i + (r_0 - r_1)\}^{3/2}} \\
& - g'(s_0) \sqrt{\frac{s_0 - s_1}{r_0 - r_1}} \sum_{k=1}^n H_k W(r_1, s_0 - (s_0 - s_1)x_k) - g'(r_0) \sqrt{\frac{r_0 - r_1}{s_0 - s_1}} \sum_{k=1}^n H_k W(r_0 - (r_0 - r_1)x_k, s_1) \\
& - g'(r_0) \frac{(r_1 - r_2)}{\sqrt{s_0 - s_1}} \sum_{i=1}^n G_i \frac{W(r_1 - (r_1 - r_2)z_i, s_1)}{\{(r_0 - r_1) + (r_1 - r_2)z_i\}^{1/2}} - g'(s_0) \frac{(s_1 - s_2)}{\sqrt{r_0 - r_1}} \sum_{i=1}^n G_i \frac{W(r_1, s_1 - (s_1 - s_2)z_i)}{\{(s_0 - s_1) + (s_1 - s_2)z_i\}^{1/2}} \\
& + g'(r_0)g'(s_1) \frac{(s_1 - s_2)}{\sqrt{r_0 - r_2}} \sum_{i=1}^n G_i \frac{W(r_2, s_1 - (s_1 - s_2)z_i)}{\{(s_0 - s_1) + (s_1 - s_2)z_i\}^{1/2}} \\
& + g'(s_0)g'(r_1) \frac{(r_1 - r_2)}{\sqrt{s_0 - s_2}} \sum_{i=1}^n G_i \frac{W(r_1 - (r_1 - r_2)z_i, s_2)}{\{(r_0 - r_1) + (r_1 - r_2)z_i\}^{1/2}}.
\end{aligned}$$

... (18)

6 APPLICATION

The analytical expressions given above for the direct evaluation of aerodynamic loading represent a convenient application of linearized thin-wing theory. A degree of approximation is adopted in so far as the formulation is based on Etkin's construction limited to two integration areas. The justification for this was discussed qualitatively in Section 2; it is now of interest to compare results with exact theory in a simple case where this can be conveniently applied. For a more general case, the results of the present method may be compared with other available theories to illustrate the measure of divergence.

6.1 Cambered delta wing

As a typical case, a cambered delta wing of aspect ratio 1.0 in steady pitch ($\frac{W}{V} = \frac{qX}{c_0}$) was examined at a Mach number of 2.0. Results were computed by the present method and by the method established by Watkins^{3,4} and applied by Davies⁵. Spanwise and chordwise distributions are shown in Figs.3 and 4. The correspondence is very close.

6.2 Uncambered ogee wing

To illustrate the application of the method to a wing with curved leading edges, the model used by Courtney and Ormrod⁶ was chosen. This is an uncambered ogee configuration of aspect ratio 1.0 and with leading edge equations:-

$$y = S_t \left[0.5 \frac{x}{c_0} + \left(\frac{x}{c_0} \right)^2 - 0.5 \left(\frac{x}{c_0} \right)^5 \right].$$

In Figs.5 and 6 spanwise and chordwise pressure distributions are shown according to the present formulation of linearized thin-wing theory for $M = 1.4, 2.0$ and 2.8 . Even at the lowest speed the difference between the present method and slender-body theory is appreciable. The divergence becomes greater at higher speeds, as would be expected from the restrictions imposed by the assumptions of slender-body theory. At the highest speed, the uniform pressure loading according to first-order piston theory does not give as useful an indication of local loadings as do the results based on the present method.

Flow visualization had shown separation from the leading edges, with vortex formation, at each of the speeds and incidences quoted in Figs.5 and 6, the effects being most marked at lower speeds and higher incidences. Further, the centre section was relatively thick. Strictly speaking, therefore, linearized thin-wing theory cannot be applied, nor the experimental values used to assess variants of linearized theory. However, the experimental points, taken from Courtney and Ormrod's paper, show that the present theory provides a useful indication of pressure distribution in regions least affected by

separation effects (inboard, high speed, low incidence). Since separation must affect pressure distribution to a greater or lesser extent at all points, it is not safe to generalise from this one case; the extent to which the conditions may depart from the basic thin wing and attached flow assumptions for the present method still to give useful results could be established only by comparison with experiment over a wide range of conditions.

ACKNOWLEDGEMENT

The author would like to thank Dr. D.E. Davies for suggesting the analytical approach used in this paper and for helpful discussions.

LIST OF SYMBOLS

A_1, A_2	integration areas
$C_p = (p - p_o) / \frac{1}{2} \rho V^2$,	pressure coefficient
$\Delta C_p = (p_l - p_u) / \frac{1}{2} \rho V^2$	
G_i, H_i	integration coefficients
M	Mach number
p	pressure
r, s	characteristic coordinates, defined in equation (5)
$r = g(s)$	equation of starboard leading edge
$s = g(r)$	equation of port leading edge
V	free stream velocity
$w(x, y)$	downwash velocity in Cartesian coordinates
$W(r, s)$	downwash velocity in characteristic coordinates
x, y, z	Cartesian coordinates
$ty = h(x)$	equation of leading edges
x_i, z_i	integration points
q	rate of pitch or equivalent camber

LIST OF SYMBOLS (CONTD)

α	incidence
β	$\sqrt{M^2 - 1}$
ρ	free stream density
$\mu = \sin^{-1} (1/M)$	(Fig.1)
ϕ, Φ	velocity potential

Suffices

o	free stream and coordinates of reference point
l	lower surface
u	upper surface

LIST OF REFERENCES

<u>No.</u>	<u>Author</u>	<u>Title, etc.</u>
1	Jones, R. T.	Properties of low-aspect-ratio pointed wings at speeds below and above the speed of sound. N.A.C.A. Rep. No.835. A.R.C.9483. 1946.
2	Lighthill, M. J.	Oscillating airfoils at high Mach number. Jnl. Aero. Sci. <u>20</u> (6) 1953.
3	Watkins, C. E. Berman, J. H.	Air forces and moments on triangular and related wings with subsonic leading edges oscillating in supersonic potential flow. N.A.C.A. Rep. No.1099. 1952.
4	Watkins, C. W. Berman, J. H.	Velocity potential and air forces associated with a triangular wing in supersonic flow with subsonic leading edges and deforming harmonically according to a general quadratic equation. N.A.C.A. Tech. Note No.3009. 1953.
5	Davies, D. E.	The velocity potential on triangular and related wings with subsonic leading edges oscillating harmonically in supersonic flow. A.R.C. R & M 3229. Feb. 1959.
6	Evvard, J. C.	Use of source distribution for evaluating theoretical aerodynamics of thin finite wings at supersonic speeds. N.A.C.A. Rep. No.951. A.R.C. 13821. 1950.

LIST OF REFERENCES (CONTD)

- | <u>No.</u> | <u>Author</u> | <u>Title, etc.</u> |
|------------|-----------------------------------|---|
| 7 | Etkin, B. | Numerical integration methods for supersonic wings in steady and oscillatory motion. Univ. of Toronto, Inst. of Aerophysics Rep. No.36, P.58440. 1955. |
| 8 | Lees, D. E. | Aerodynamic influence coefficients for delta wings in steady supersonic flow. Aircraft Engineering, <u>31</u> (359) 1959. |
| 9 | Courtney, A. L.
Ormerod, A. O. | Pressure plotting and force tests at Mach numbers up to 2.8 on an uncambered slender wing of $p = \frac{1}{2}$, $s/c = \frac{1}{4}$. ("Handley Page Ogee"). R.A.E. Tech. Note No. Aero 2760. A.R.C. 23,109. 1961. |
| 10 | Edwards, J. | A treatise on the integral calculus (Chap.X). Macmillan & Co. 1930. |
| 11 | Mineur, H. | Technique de calcul numerique. Librairie Polytechnique Ch. Beranger. 1952. |

APPENDIX 1

REMOVAL OF SINGULARITY FROM DOUBLE INTEGRAL

In order to remove the singularity in the double integral of equation (10), consider the integral

$$\begin{aligned} & \frac{1}{2} \int_{s_0}^{s_1} \frac{ds}{\sqrt{s_0 - s}} \int_t^{r_1} \frac{\frac{dt}{dr_0} W(t,s) dr}{(r_0 - r)^{3/2}} \\ &= \frac{dt}{dr_0} \int_{s_0}^{s_1} \frac{W(t,s) ds}{\sqrt{s_0 - s}} \left[\frac{1}{\sqrt{r_0 - r_1}} - \frac{1}{\sqrt{r_0 - t}} \right] \\ &= - \frac{dt}{dr_0} \frac{1}{\sqrt{r_0 - t}} \int_{s_0}^{s_1} \frac{W(t,s) ds}{\sqrt{s_0 - s}} + \frac{dt}{dr_0} \frac{1}{\sqrt{r_0 - r_1}} \int_{s_0}^{s_1} \frac{W(t,s) ds}{\sqrt{s_0 - s}} . \end{aligned}$$

Therefore,

$$\begin{aligned} & \frac{dt}{dr_0} \frac{1}{\sqrt{r_0 - t}} \int_{s_0}^{s_1} \frac{W(t,s) ds}{\sqrt{s_0 - s}} \\ &= - \frac{1}{2} \int_{s_0}^{s_1} \frac{ds}{\sqrt{s_0 - s}} \int_t^{r_1} \frac{\frac{dt}{dr_0} W(t,s) dr}{(r_0 - r)^{3/2}} + \frac{dt}{dr_0} \frac{1}{\sqrt{r_0 - r_1}} \int_{s_0}^{s_1} \frac{W(t,s) ds}{\sqrt{s_0 - s}} . \end{aligned}$$

Substitution in Equation (10) then leads to the expression given in Equation (11).

APPENDIX 2

CALCULATION OF TANGENTS AT POINTS OF INTERSECTION

The equation of the leading edge is usually given in Cartesian coordinates. We therefore want to express the values of $g'(r_0)$ etc. in terms of the equation in Cartesian coordinates without working out the equation of the leading edge explicitly in characteristic coordinates.

Let the equation of the starboard leading edge be

$$y = a_0 + a_1 x + a_2 x^2 + \dots + a_n x^n = h(x)$$

or replacing y by its equivalent in characteristic coordinates

$$\frac{1}{M} (s - r) = \frac{1}{M} \{s - g(s)\} = h(x) .$$

Differentiating with respect to s we get

$$\frac{1}{M} \{1 - g'(s)\} = \frac{dh}{dx} \frac{dx}{ds}$$

On the leading edge $x = \frac{\beta}{M} \{s + g(s)\}$ so that

$$\frac{1}{M} \{1 - g'(s)\} = h'(x) \frac{\beta}{M} \{1 + g'(s)\}$$

therefore
$$g'(s) = \frac{1 - \beta h'(x)}{1 + \beta h'(x)} .$$

The port leading edge is given by $-y = h(x)$, which leads to

$$\frac{1}{M} (r - s) = \frac{1}{M} \{r - g(r)\} = h(x) .$$

Differentiating with respect to r we get

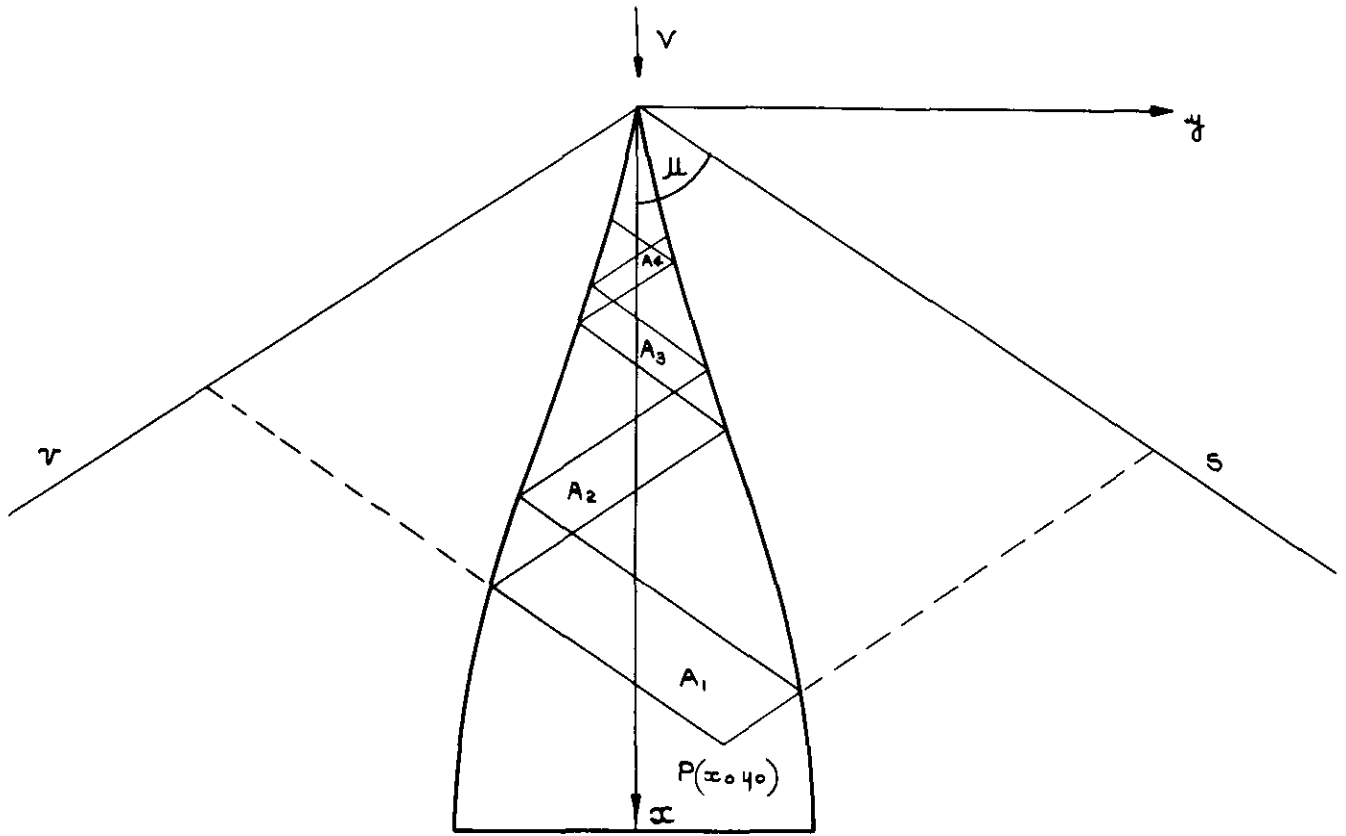
$$g'(r) = \frac{1 - \beta h'(x)}{1 + \beta h'(x)} .$$

Thus $g'(r)$ and $g'(s)$ are expressed in terms of $h'(x)$, but we must be careful to refer to the right points since $h'(x)$ contains r as well as s of the point in question. The point P does not lie on the leading edge, but $r_P = r_R = r_0$ and $s_P = s_Q = s_0$ (see Fig.2). Hence $g'(r_0)$ refers to the tangent at R ; similarly $g'(s_0)$, $g'(r_1)$, $g'(s_1)$ refer to the tangents at Q , T and U respectively.

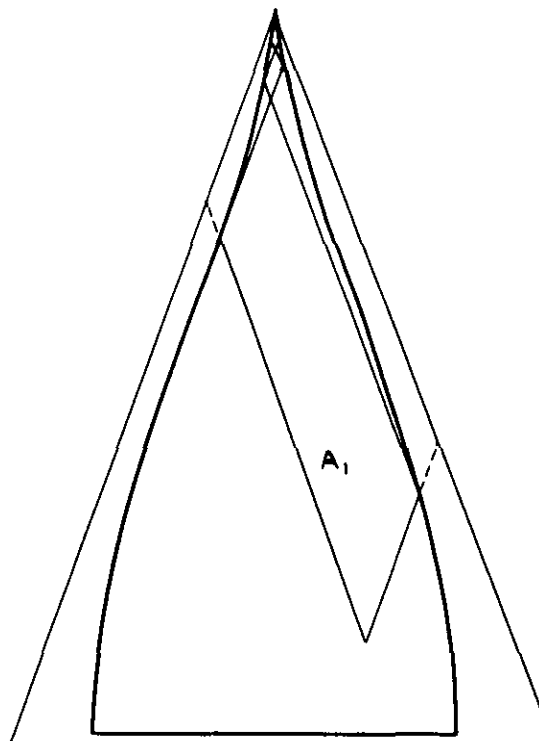
TABLE 1

Integration points and interpolation
coefficients for Gaussian integration

$i(\equiv k)$	x_i	H_i	z_i	G_i
1	0.015683	0.498294	0.0337652	0.085662
2	0.135300	0.466985	0.1693953	0.180381
3	0.344942	0.406335	0.3806904	0.233957
4	0.592750	0.320157	0.6193096	0.233957
5	0.817428	0.213879	0.8306047	0.180381
6	0.963431	0.094351	0.9662348	0.085662



(a.) INTEGRATION AREAS $M = 1.2$



(b.) INTEGRATION AREAS $M = 2.8$

FIG. I. INTEGRATION AREAS FOR A TYPICAL OGEE WING.

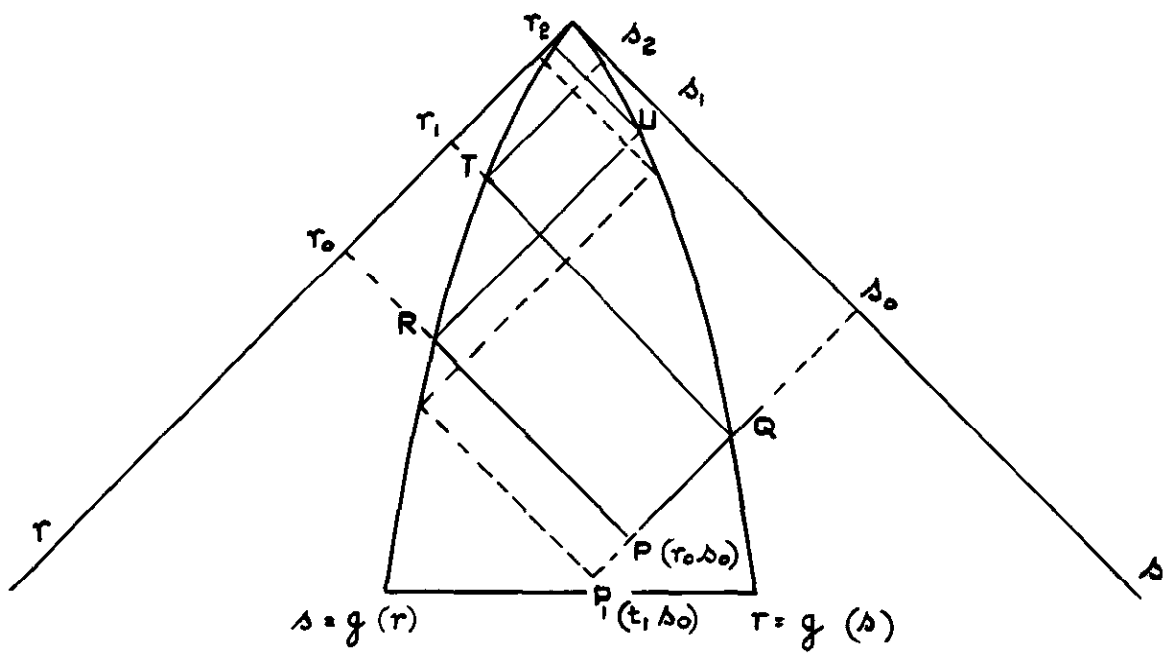


FIG. 2. NOTATION FOR COMPUTATION.

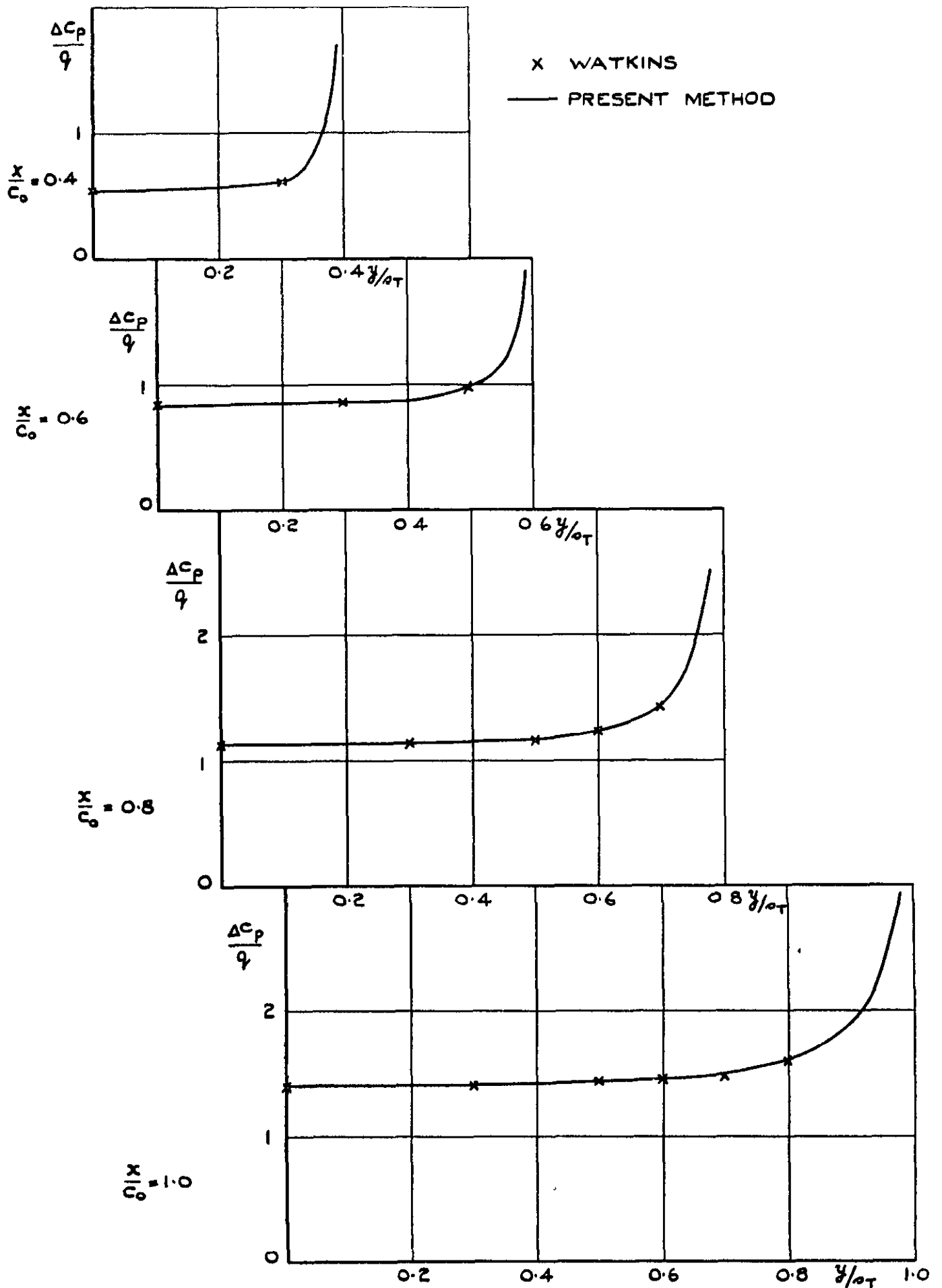


FIG.3. SPANWISE PRESSURE DISTRIBUTION. CAMBERED DELTA WING,
 $\frac{W}{V} = \frac{q x}{c_0}, M = 2.0.$

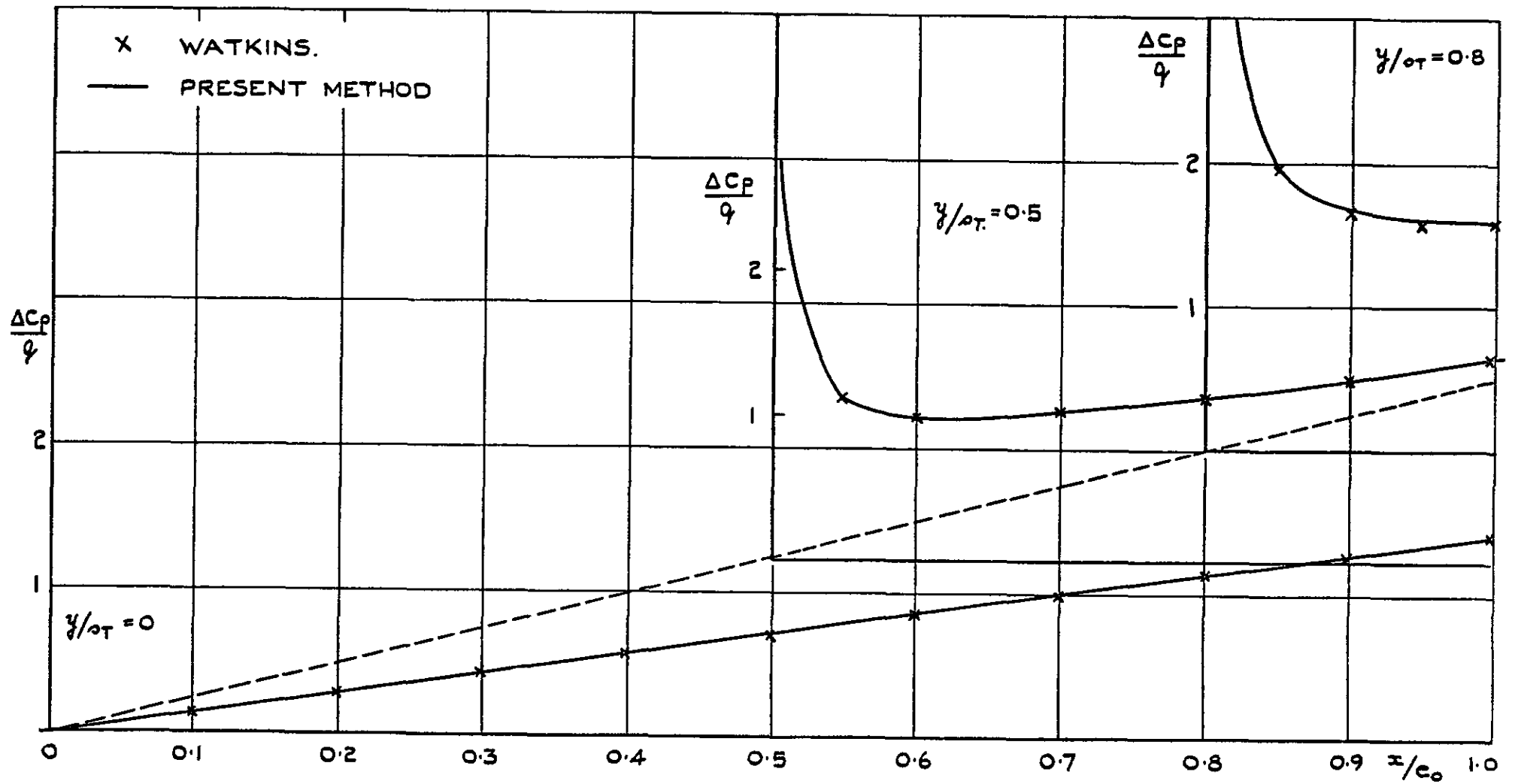


FIG. 4. CHORDWISE PRESSURE DISTRIBUTION. CAMBERED DELTA WING, $\frac{W}{V} = \frac{q x}{c_0}$, $M = 2.0$.

FIG. 4.

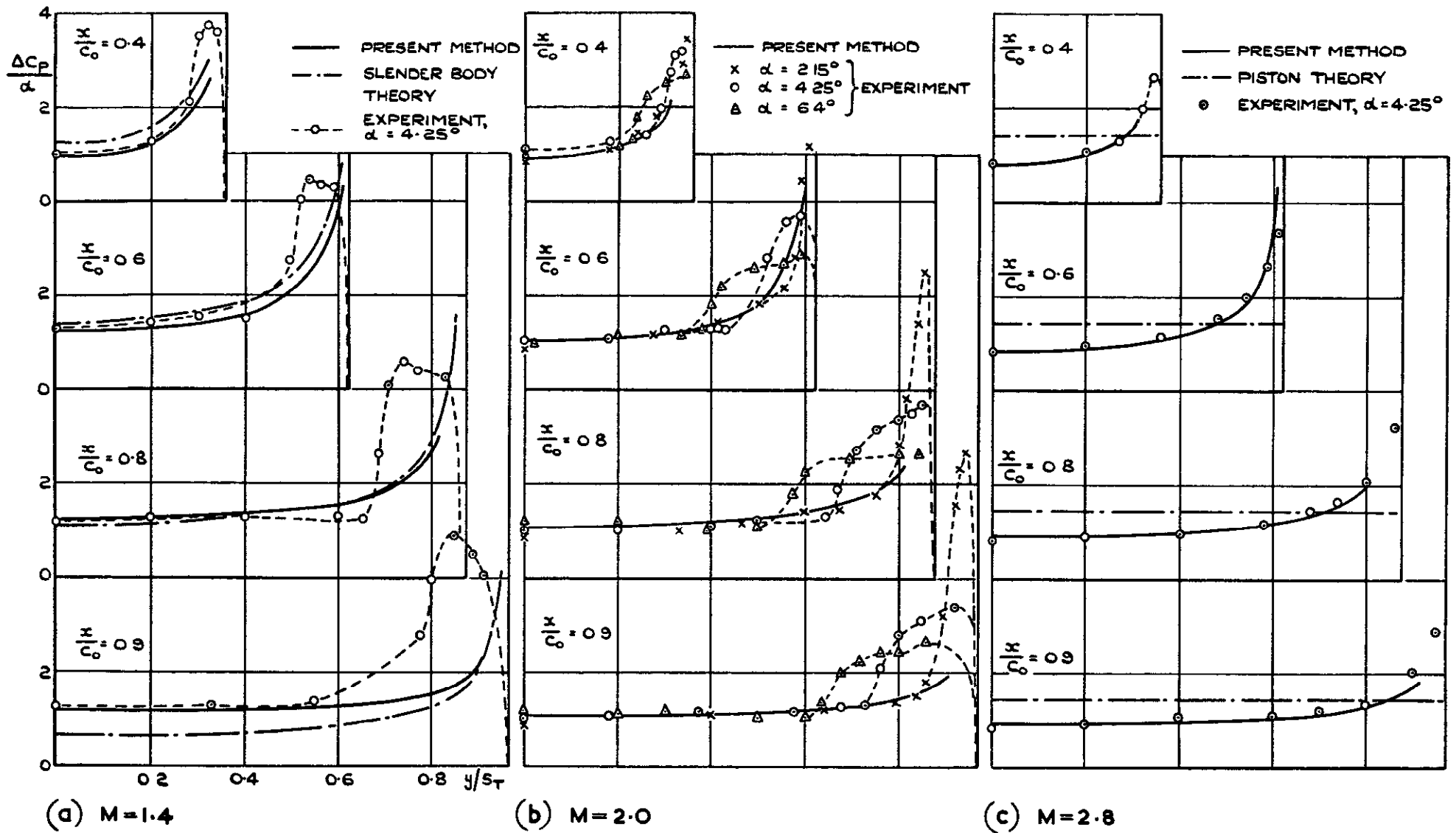


FIG.5. COMPARISON OF PRESENT METHOD WITH EXPERIMENT, SLENDER BODY THEORY AT $M=1.4$, AND PISTON THEORY AT $M=2.8$, Ogee WING SPANWISE DISTRIBUTION OF $\Delta C_p / \alpha$.

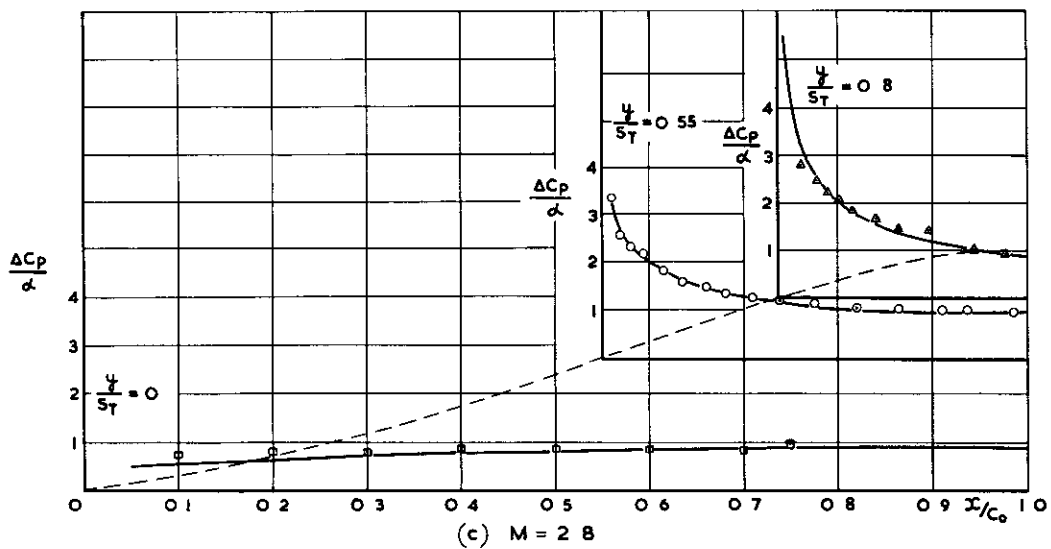
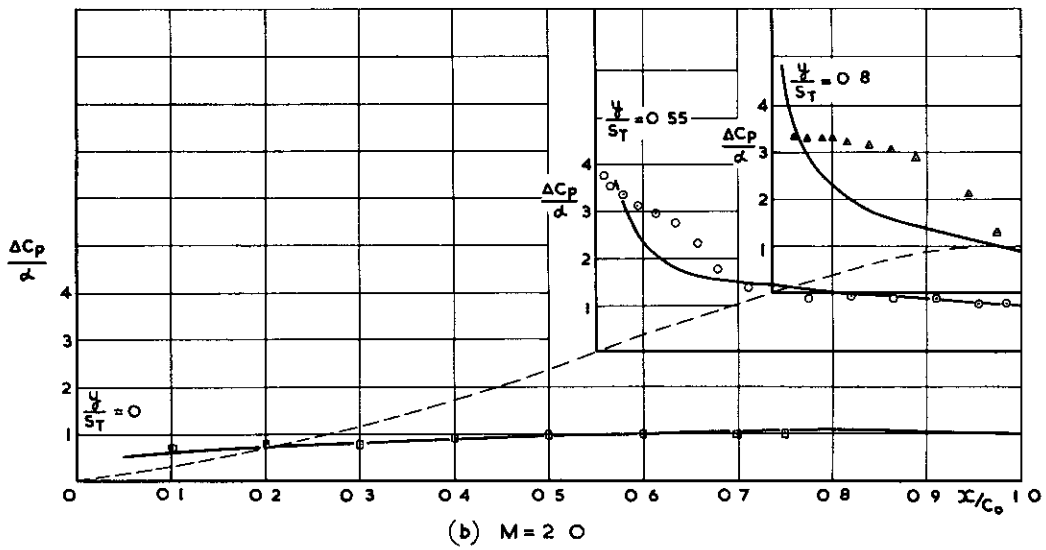
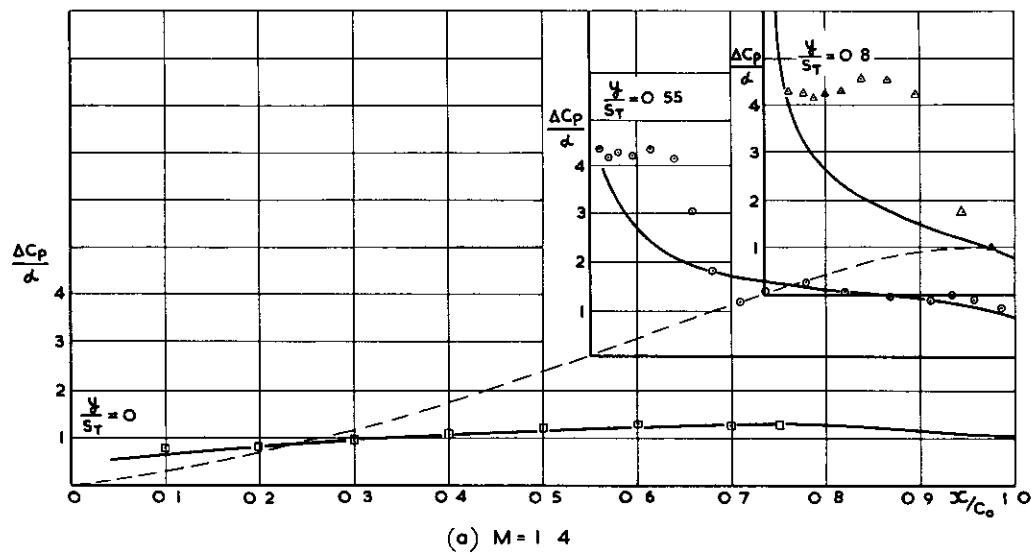


FIG. 6 CHORDWISE DISTRIBUTION OF $\Delta C_p/\alpha$ FOR OEGEE WING. COMPARISON WITH EXPERIMENT, $\alpha = 4.25^\circ$

A.R.C. C.P. No. 703

533.693.3:
533.6.048.2/3:
533.6.011.5

THE CALCULATION OF PRESSURE DISTRIBUTION IN STEADY SUPERSONIC FLOW, WITH ARBITRARY DOWNWASH DISTRIBUTION. Klanfer, L. April, 1963.

A method is established on the basis of linearized thin-wing theory for the calculation of pressure distribution, in steady supersonic flow, on wings of arbitrary planform with subsonic leading edges. An algebraic expression is derived by exact integration for the incidence contribution and a computational formula, based on Gaussian integration, is given for the general case including any prescribed camber and twist.

P.t.O.

A.R.C. C.P. No. 703

533.693.3:
533.6.048.2/3:
533.6.011.5

THE CALCULATION OF PRESSURE DISTRIBUTION IN STEADY SUPERSONIC FLOW, WITH ARBITRARY DOWNWASH DISTRIBUTION. Klanfer, L. April, 1963.

A method is established on the basis of linearized thin-wing theory for the calculation of pressure distribution, in steady supersonic flow, on wings of arbitrary planform with subsonic leading edges. An algebraic expression is derived by exact integration for the incidence contribution and a computational formula, based on Gaussian integration, is given for the general case including any prescribed camber and twist.

P.t.O.

A.R.C. C.P. No. 703

533.693.3:
533.6.048.2/3:
533.6.011.5

THE CALCULATION OF PRESSURE DISTRIBUTION IN STEADY SUPERSONIC FLOW, WITH ARBITRARY DOWNWASH DISTRIBUTION. Klanfer, L. April, 1963.

A method is established on the basis of linearized thin-wing theory for the calculation of pressure distribution, in steady supersonic flow, on wings of arbitrary planform with subsonic leading edges. An algebraic expression is derived by exact integration for the incidence contribution and a computational formula, based on Gaussian integration, is given for the general case including any prescribed camber and twist.

P.t.O.

For a uniformly cambered delta wing the results computed by this method check very closely against those obtained by Watkins' method which is applicable in this special case. As illustrated by results computed for an uncambered ogee wing the method appears to give results of more general application than slender body or first-order piston theory.

For a uniformly cambered delta wing the results computed by this method check very closely against those obtained by Watkins' method which is applicable in this special case. As illustrated by results computed for an uncambered ogee wing the method appears to give results of more general application than slender body or first-order piston theory.

For a uniformly cambered delta wing the results computed by this method check very closely against those obtained by Watkins' method which is applicable in this special case. As illustrated by results computed for an uncambered ogee wing the method appears to give results of more general application than slender body or first-order piston theory.

© *Crown copyright 1965*

Printed and published by

HER MAJESTY'S STATIONERY OFFICE

To be purchased from

York House, Kingsway, London w c 2

423 Oxford Street, London w.1

13A Castle Street, Edinburgh 2

109 St. Mary Street, Cardiff

39 King Street, Manchester 2

50 Fairfax Street, Bristol 1

35 Smallbrook, Ringway, Birmingham 5

80 Chichester Street, Belfast 1

or through any bookseller

Printed in England